1-1-2008

Birefringence and transmission of an antireflection-coated sulfur-free cadmium selenide Wollaston prism at 30 K

Christopher Packham

Rachel E. Mason

Glenn D. Boreman
University of Central Florida

Recommended Citation

Packham, Christopher; Mason, Rachel E.; and Boreman, Glenn D., "Birefringence and transmission of an antireflection-coated sulfur-free cadmium selenide Wollaston prism at 30 K" (2008). *Faculty Bibliography 2000s*. 806.
https://stars.library.ucf.edu/facultybib2000/806

University of
Central Florida

STARS
Showcase of Text, Archives, Research & Scholarship

Birefringence and transmission of an antireflection-coated sulfur-free cadmium selenide Wollaston prism at 30 K

Christopher Packham, MEMBER SPIE
University of Florida
Department of Astronomy
211 Bryant Space Science Center
P.O. Box 112055
Gainesville, Florida 32611-2055

Rachel E. Mason, MEMBER SPIE
Gemini Observatory
Northern Operations Center
670 North A'ohuku Place
Hilo, Hawaii 96720

Glenn D. Boreman, FELLOW SPIE
University of Central Florida
College of Optics & Photonics: CREOL
P.O. Box 162700
Orlando, Florida 32816-2700

Abstract. We present a determination of the change with temperature and wavelength of the degree of birefringence of a cold ($\sim$30 K) Wollaston prism constructed from antireflection (AR)–coated sulfur-free cadmium selenide (CdSe). We compare the normalized birefringence for the material to that estimated by the Sellmeier-4 formula and to previously published measurements of a warm sample of sulfur-free CdSe. Finally, we measure the transmission as a function of wavelength. *© 2008 Society of Photo-Optical Instrumentation Engineers.* [DOI: 10.1117/1.3050420]

1 Introduction

Dual-beam polarimetry using Wollaston prisms at optical and near-infrared (NIR) wavelengths[1] has been successfully employed by night-time astrophysicists to explore a variety of objects. The advantage of dual-beam polarimeters over that of their single-beam counterparts is that they produce simultaneous images in orthogonally polarized states, minimizing temporal effects of transparency, background emission, and point spread function (PSF) variations. This typically leads to a significantly higher degree of accuracy in the derived degree and position angle of polarization, as well as a greater sensitivity in a given observing time. Objects observed by dual-beam polarimeters have included debris disks around nearby stars (e.g., β Pictoris[2]), star formation regions (e.g., the core region of the Orion Molecular Cloud,[3]) and distant active galactic nuclei (AGN, e.g., NGC1068[4]). Such observations spurred key advances to our knowledge of star formation and AGN, ensuring that polarimeters are readily available on 4-m class ground-based telescopes, such as ISIS on the WHT and IRPOL2 on UKIRT. However, as noted by Hough,[5] the escalating use of adaptive optics and the increasing competition for the Cassegrain focus on the 8-m class of telescopes may have led to the relative lack of facility-class polarimeters on these telescopes, with the notable exception of ESO's VLT instrumentation suite.

On the 8.1-m Gemini North telescope, the mid-infrared (MIR) instrument Michelle[6] is equipped with a polarimetric mode, employing an external (hence room temperature) half-wave retarder as the modulator, located upstream of the dewar entrance window. Interior to the dewar is a wire grid polarizer, operating as the polarimetric analyzer. While this represents the first operational MIR polarimeter on an 8-m class telescope, it is a single-beam device and is therefore susceptible to the often rapid changes in transparency and background emission typical at MIR wavelengths. Nevertheless, early results from the polarimetry mode of Michelle[7] are indicative of the scientific promise this technique holds. New instruments on advanced observatories, such as the SOFIA airborne observatory, hold the promise of further advances from the ground. Recently, Packham et al.[8,9] have proposed a dual-beam 5- 40-μm polarimeter for SOFIA, an instrument that would provide the observatory with a unique scientific legacy.

The CanariCam 7.5-μm to 26-μm imager, spectrometer, polarimeter, and coronagraph[10] recently completed at the University of Florida's Department of Astronomy incorporates, for the first time at these wavelengths, a dual-beam polarimetric design.[11] The detector is an arsenic-doped silicon, blocked-impurity-band (BIB) device from Raytheon, with peak quantum efficiency (QE) in the 8- to 25-μm region and a rapid decrease in QE at longer wavelengths. Integral to the CanariCam design is a Wollaston prism (built by Cleveland Crystals, http://www.clevelandcrystals.com) constructed from sulfur-free cadmium selenide (CdSe), located interior to the CanariCam dewar, upstream of one of four selectable diffraction gratings or the primary imaging mirror. This gives CanariCam the ability to make dual-beam polarimetric observations in both imaging and spectroscopic modes, taking advantage of the benefits already realized at optical and NIR wavelengths. The unfolded optical layout of CanariCam is shown in Fig. 1. Because the Wollaston prism is located
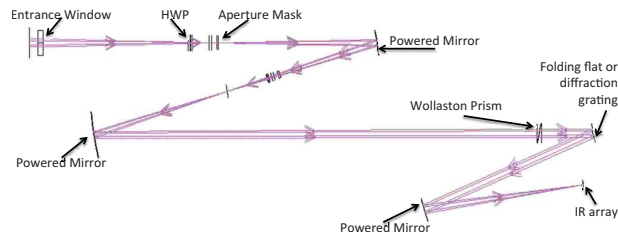
Fig. 1 Unfolded CanariCam optical layout.

inside the CanariCam Dewar, it is at a temperature of ~30 K. The Wollaston prism is coated on all optical surfaces with an antireflection (AR) coating, optimized for equal ordinary and extraordinary ray transmission across the N band window, with a peak transmission at 9.5 μm. Each of the Wollaston prism halves is 33×38 mm on the "flat" face, has a minimum and maximum thickness of 2.5 mm and 9.4 mm, respectively, and has a cut angle of 10.3 deg. All edges are beveled to eliminate stress points during cooling. Detailed descriptions of the instrument can be found in Packham et al.[11,12] and Telesco et al.[10]

The design of the Wollaston prism was achieved through Zemax modeling and use of the Sellmeier-4 formula, using values obtained from the *Handbook of Optics*, vol. 2.[13] Estimates of the birefringence of CdSe as a function of wavelength were made, providing the polarimetric dispersion [separation of the ordinary (o) and extraordinary (e) rays] versus wavelength. In this paper, we report on the accuracy and applicability of the Sellmeier-4 formula to a sulfur-free CdSe Wollaston prism at ~30 K. The second aim of this paper is to report on the transmission of the Wollaston through our operational wavelengths of CanariCam (~7 to 26 μm).

2 Imaging Polarimetry

Wollaston prisms, which produce an angular separation between the ordinary and extraordinary rays, have been used in the collimated beams of NIR cameras and spectrometers (e.g., Ref. 14). The angular deviation (δ_{eo}) of the two emergent beams is provided by:

$$\delta_{eo} = 2(n_e - n_o) \times \tan \Omega,$$

where Ω is the prism angle, and $(n_e - n_o)$ is the material birefringence.

The material selection for the Wollaston prism should consider the transmission, required beam separation, and wavelength dependence of birefringence (images elongate in the polarization dispersion direction), especially when used in high spatial resolution and broadband applications. Where optical cements are available, it is usual to optically contact the two components of the Wollaston prism. However, for CanariCam, no such cements were available, and instead there is a small gap (<0.5 mm) between the Wollaston sections.

To measure the wavelength dependence of the birefringence of the Wollaston prism, we placed a mask with two circular apertures at the telescope focal plane, which was back-illuminated by an effectively unpolarized blackbody source at room temperature. (Two apertures were not re-

Table 1 Measured polarimetric dispersion versus wavelength.

Filter name	λc (μm)	$\delta\lambda$ (μm)	Normalized dispersion
M	4.70	0.55	0.9995
Si1	7.80	1.10	0.9986
PAH1	8.60	0.43	1.000
Si2	8.70	1.10	0.9876
ArIII	8.99	0.13	0.9797
Si3	9.80	1.00	0.9697
Si4	10.30	0.90	0.9622
N	10.36	5.20	0.9105
SIV	10.52	0.16	0.9684
PAH2	11.30	0.60	0.9450
Si5	11.60	0.90	0.9549
SiC	11.75	2.50	0.8903
Si6	12.50	0.70	0.9251
NeII	12.81	0.20	0.9262
NeII_ref2	13.10	0.20	0.9109
QH2	17.00	0.40	0.7763
Q1	17.65	0.90	0.7518
Q4	20.50	1.00	0.6768
Qw	20.90	8.80	0.7015
Q8	24.50	0.80	0.5463

quired for the purposes of this experiment, but the two-aperture mask was installed for other instrument characterization purposes. By having two apertures, errors in the final results were reduced, and we use both apertures throughout this paper.) We inserted the Wollaston prism into the science beam and measured the distance between the resultant image centroids on the array. This was repeated for each filter, and the results are reported in Table 1, where λ_c is the central wavelength of the filter, and $\delta\lambda$ is the filter bandwidth, expressed in μm. We calculate the expected index of refraction, n_o and n_e for the ordinary and extraordinary rays, respectively, using the Sellmeier-4 formula shown here, taking the constants A, B, C, D, and E from the *Handbook of Optics*, vol. 2,[13] as listed in Table 2.

$$n^2 = A + \frac{B\lambda^2}{\lambda^2 - C} + \frac{D\lambda^2}{\lambda^2 - E}$$

We normalize that value to 8.6 μm (the shortest central wavelength of a narrow-band filter and where spectropolarimetric data is available; see Sec. 3). The predicted nor-

Table 2 Sellmeier-4 parameters for CdSe.

CdSe	A	B	C	D	E
Ordinary	4.2243	1.7680	0.2270	3.1200	3380
Extraordinary	4.2009	1.8875	0.2171	3.6461	3629

malized (also at 8.6 μm) birefringence is presented in Table 3, and a normalized comparison between the predicted and measured birefringence is shown in Fig. 2.

Figure 2 shows that the Sellmeier-4 formula estimates the birefringence of the CdSe Wollaston to within 6.4% for all filters, with the maximum deviation occurring for our N band ($\lambda_c = 10.36$ μm) filter. However, the predicted birefringence using the Sellmeier-4 formula assumes a monochromatic input, whereas the filters used in CanariCam have a variable bandwidth, and three of them have a sig-

Table 3 Predicted birefringence versus monochromatic wavelength using Sellmeier-4 formula a.

Wavelength (μm)	Birefringence (—)	Normalized birefringence (—)
4.70	0.0193	1.0445
7.80	0.0186	1.0110
8.60	0.0184	1.0000
8.70	0.0184	0.9986
8.99	0.0183	0.9943
9.80	0.0181	0.9815
10.30	0.0179	0.9731
10.36	0.0179	0.9721
10.52	0.0179	0.9693
11.30	0.0176	0.9550
11.60	0.0175	0.9493
11.75	0.0175	0.9464
12.50	0.0172	0.9311
12.81	0.0171	0.9245
13.10	0.0169	0.9182
17.00	0.0151	0.8188
17.65	0.0147	0.7996
20.50	0.0130	0.7068
20.90	0.0128	0.6926
24.50	0.0102	0.5540

nificantly broader bandwidth than the others. The N band filter has the largest bandwidth (5.2 μm) that is fully transmissive through the Wollaston (see Sec. 3.2) and shows the greatest divergence from the monochromatically calculated birefringence. The Qw filter ($\lambda_c = 20.9$ μm) has an 8.8-μm bandwidth, but at the longest wavelengths the Wollaston is poorly transmissive or opaque, giving an effective bandwidth of ~6 μm, and biased toward shorter wavelengths due to the Wollaston transmission profile (see Sec. 3.2). The SiC filter ($\lambda_c = 11.75$ μm) has the third widest bandwidth (2.5 μm) and similarly shows a significant deviation from the Sellmeier-4 formula. With the exclusion of these three filters, a trend to a higher absolute discrepancy between the measured and estimated birefringence can be seen at both shorter and longer wavelengths than the normalization point (8.6 μm), but the magnitude of that discrepancy is difficult to estimate due to the variable and chromatic bandwidths of the filters. To investigate the birefringence at a finer spectral resolution to reduce chromatic effects, we repeated the experiment in spectropolarimetry mode.

3 Spectropolarimetry

CanariCam has the provision to make spectro- and imaging-polarimetric observations, using standard diffraction gratings. As the introduction of diffraction gratings typically polarizes light, the Wollaston prism is located upstream of the grating, so any polarization effects introduced by the grating will have a negligible effect on the measured intensity of ordinary and extraordinary beams. We measure the polarimetric dispersion as a function of wavelength, using the N or Qw filters as spectroscopic order blocking filters. The wavelength coverage is less in spectropolarimetic mode compared to imaging polarimetry mode, as the grating design permits spectroscopy only within the bandpasses of the N and Qw filters, whereas imaging can be performed at wavelengths as short as $\lambda_c = 4.7$ μm. The spectral resolutions at the central wavelengths of the N and Qw filters are ($\lambda / \delta\lambda$) 175 and 120, respectively.

A constant temperature, effectively unpolarized, blackbody source was used to illuminate the two circular apertures in the focal plane mask. We perform wavelength calibration through introduction of a laboratory-characterized thin film of polystyrene located within the instrument. This film has several absorption lines through the N band filter and thus enables accurate wavelength calibration of the instrument. In the case of the Qw filter, we use the central wavelengths of the narrow band filters Q1, Q4, and Q8 to obtain an approximate wavelength calibration. In the N band filter, the wavelength calibration has an uncertainty of ~0.02 μm as estimated from the root mean square (rms) of the final wavelength calibration fitting of five absorption lines from the polystyrene. The uncertainty in the polarimetric dispersion is estimated from that of the centroid routine and is estimated to be a constant 0.1 pixels for each spectrum, or 0.67% in the smallest polarimetric dispersion.

3.1 Birefringence

The normalized polarimetric dispersion versus wavelength is shown in Fig. 3 for the entire N and Qw band windows. We also plot the dispersion estimated from the Sellmeier-4
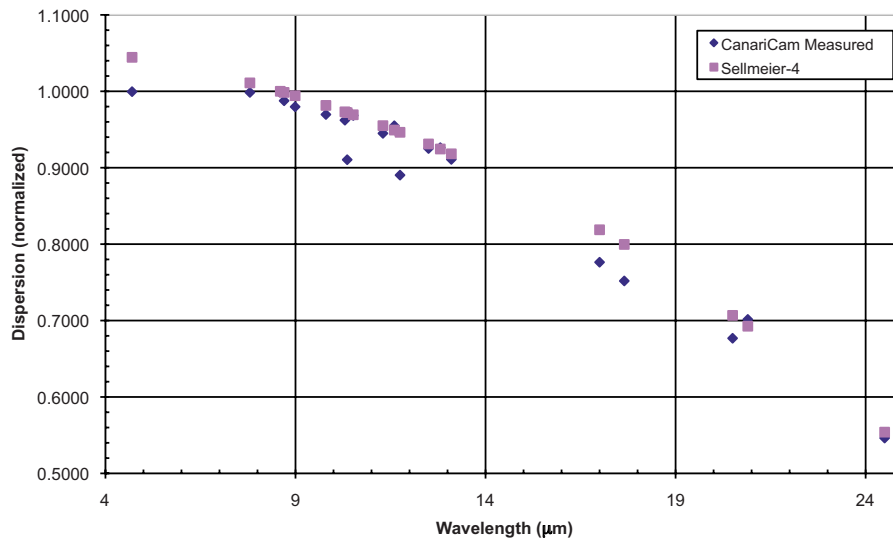
Fig. 2 Normalized birefringence versus wavelength using Sellmeier-4 formula.

formula on the same graph, also normalized to 8.5 μm. We normalize to 8.5 μm, as this is the shortest wavelength at which both CanariCam dispersion values and those from a room temperature sample of CdSe characterized by Chenault and Chipman[15] are available. This wavelength is also very close to that used for the normalization of the preceding imaging observations.

We tabulate the percentage deviation from the measured polarimetric dispersion from that estimated by the Sellmeier-4 formula in Table 4, showing that the Sellmeier-4 formula predicts the dispersion to <2.1% across the N band filter but predicts values as much as 11.76% different in the Qw band filter for the cold AR-coated Wollaston. While the existing data does not directly provide the birefringence, if the 8.5-μm birefringence estimated by the Sellmeier-4 formula is correct for our cold Wollaston prism, we can estimate it based on our values of the normalized polarimetric dispersion also at 8.5 μm. Table 4 also lists our calculated birefringence for our cold Wollaston prism based on this assumption.

We also compared the birefringence of the cold Wollaston prism to the sample of room temperature ($\sim$293 K),

sulfur-free CdSe measured by Chenault and Chipman.[15] Figure 4 shows the birefringence measurements for the two samples, plotted as a function of deviation from the Sellmeier-4 formula to the longest wavelength measured by Chenault and Chipman.[15] The deviation from the Sellmeier-4 formula is significantly greater for the cold sample, and we note that the trend to a lower dispersion between the measured and estimated birefringence from that estimated from the Sellmeier-4 formula occurs at shorter wavelengths for the cold sample.

3.2 Transmission

CanariCam allows the accurate measurement of transmission versus wavelength for the AR-coated CdSe Wollaston prism up to $\sim$26 μm, allowing one to determine accurately the long wavelength cutoff of CdSe at 30 K. The Wollaston transmission is calculated by first adding the wavelength-calibrated ordinary and extraordinary spectra (S_1). The Wollaston prism is then removed from the optical path, and a second spectrum (ordinary ray only) is recorded and wavelength calibrated as before (S_2). Last, a ratio of the
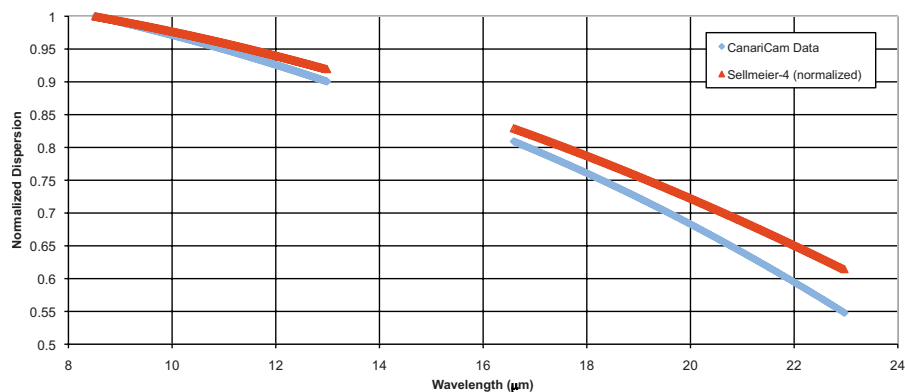

Fig. 3 Normalized birefringence versus wavelength for the N and Qw bands as measured from the spectropolarimetric data.

Table 4 Wavelength versus deviation from the Sellmeier-4 formula for the cold Wollaston prism and the calculated birefringence.

Wavelength (μm)	% Deviation (—)	Birefringence (—)
22.84	−11.76%	0.01022
22.55	−10.94%	0.01049
22.26	−10.19%	0.01074
21.97	−9.49%	0.01100
21.68	−8.84%	0.01125
21.38	−8.24%	0.01152
21.09	−7.68%	0.01173
20.80	−7.15%	0.01199
20.51	−6.66%	0.01223
20.22	−6.21%	0.01243
19.93	−5.78%	0.01266
19.64	−5.38%	0.01288
19.34	−5.01%	0.01312
19.05	−4.66%	0.01333
18.76	−4.34%	0.01352
18.47	−4.03%	0.01372
18.18	−3.75%	0.01392
17.89	−3.48%	0.01411
17.60	−3.23%	0.01431
17.31	−3.00%	0.01449
17.01	−2.79%	0.01469
16.72	−2.59%	0.01487
12.90	−2.05%	0.01668
12.71	−1.94%	0.01677
12.52	−1.83%	0.01685
12.33	−1.73%	0.01694
12.14	−1.62%	0.01703
11.94	−1.52%	0.01713
11.75	−1.42%	0.01722
11.56	−1.32%	0.01729
11.37	−1.22%	0.01738
11.18	−1.13%	0.01746

Table 4 (*Continued.*)

Wavelength (μm)	% Deviation (—)	Birefringence (—)
10.98	−1.04%	0.01755
10.79	−0.94%	0.01762
10.60	−0.86%	0.01770
10.41	−0.77%	0.01777
10.30	−0.68%	0.01782
10.02	−0.60%	0.01793
9.83	−0.52%	0.01801
9.64	−0.44%	0.01807
9.45	−0.36%	0.01814
9.26	−0.28%	0.01821
9.06	−0.21%	0.01828
8.87	−0.13%	0.01835
8.68	−0.06%	0.01841
8.49	0.01%	0.01847
8.30	0.08%	0.01854

resulting spectra (S_2/S_1) is made. As a ratio was taken and the only difference in the instrument setup was the Wollaston prism, the transmission of the instrument (filter, grating blaze, detector response, etc.) is removed.

The transmission versus wavelength for the combined N and Qw filters is shown in Figure 5 for all values where the combined filter and Wollaston transmission is >5%. As the pixel wells were deeply filled across the spectra but negligibly filled in the area outside the spectra, below 5% transmission the calculated birefringence could be affected by so-called cross-talk effects intrinsic to the array,[16] degrading the signal-to-noise ratio (SNR). The transmission of the CdSe Wollaston is modified by the AR coating, which is placed on the four optical surfaces of the Wollaston (both the interior and exterior surfaces). Special attention was paid to optimizing the AR coating to provide a balanced transmission of orthogonally polarized light at 9.5 μm. At the 50% cut-on of the N band filter (~7.7 μm), the transmission of the AR coating alone is ~97%, reaching a maximum of ~99.8% at 9.5 μm, falling back to ~96% at the cutoff of the N band filter (~13.0 μm). At 20 μm, the AR coating transmission is ~89%. The transmission of the AR–coated Wollaston prism in the N band window shows the modification to the transmission due to the AR coating, reaching a maximum transmission of 90.6% at 10.21 μm. At wavelengths >16 μm, the variation in transmission is consistent with Fabry-Pérot type interference due to the increased reflectance outside the optimum design range of the AR coatings on the optical surfaces defining the air space,
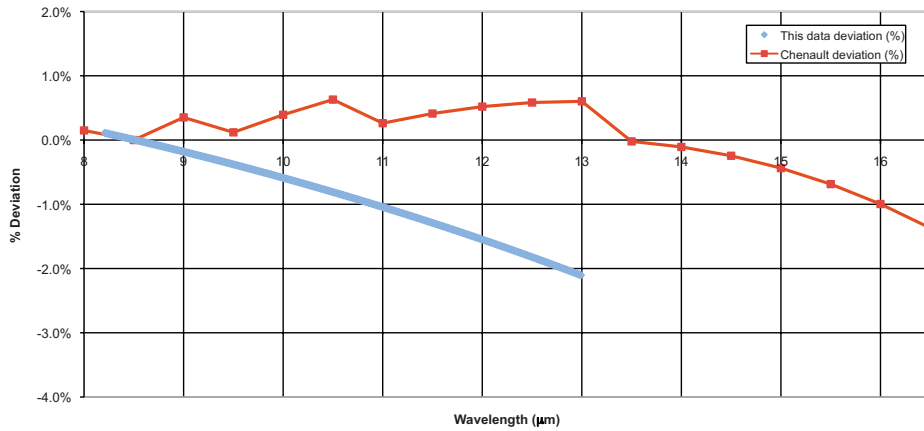
Fig. 4 Deviation from Sellmeier-4 formula versus wavelength.

leading to the rapidly varying transmission profile. Despite this, we note that the transmission is >15% up to 23.3 μm. Wavelengths ≳23.3 μm are within the Qw filter, and the detector maintains sensitivity up to ~26 μm, so the long wavelength cutoff must be due to the CdSe Wollaston and/or the AR coating.

4 Discussion

We find that the Sellmeier-4 formula shows a significant (>5%) deviation from that measured for the CanariCam Wollaston at all wavelengths >19.3 μm, based on our normalization to 8.5 μm. As we are comparing dispersions normalized to 8.5 μm, it remains uncertain wheather the deviation in dispersion between theory and that measured occurs at short or long wavelengths. However, as the deviation of dispersions shows a increasing gradient toward longer wavelengths, the normalization to 8.5 μm in the measured dispersion likely provides the most representative values. The parameters for the Sellmeier-4 formula were

determined for CdSe at temperatures much higher than our cold Wollaston sample, at around room temperature (~300 K). It is reasonable to attribute the discrepancy between our measurements and the Sellmeier-4 formula to temperature effects leading to a contraction in the crystalline structure of the CanariCam CdSe Wollaston. The significant change in birefringence for the cold sample as compared to the warm sample of Chenault and Chipman[15] strongly supports this hypothesis.

The transmission of the cold AR-coated Wollaston prism shows good performance (>70% transmission) through the optimized design wavelengths, and further shows significant transmission at wavelengths up to ~23 μm. The spectral transmission scan of warm sulfur-free CdSe performed by Cleveland Crystals[17] shows that the transmission falls to 50% of the peak at ~23 μm and then falls precipitously at longer wavelengths. The transmission of the AR-coated Wollaston falls to 50% of the longest wavelength peak transmission at 23.2 μm, a wavelength that is within the
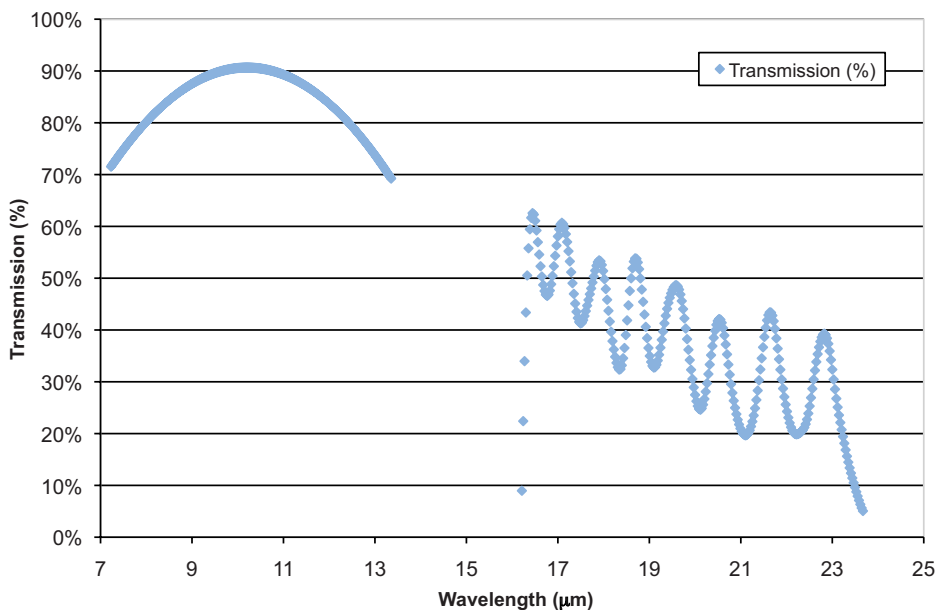

Fig. 5 Wollaston transmission versus wavelength.

errors of the warm measurements. Therefore, the cooling of the material has little or no effect on the long-wavelength cutoff of transmission.

5 Conclusions

We have measured the polarimetric dispersion and total transmission of an AR-coated, sulfur-free CdSe Wollaston at ~30 K. We find that the polarimetric dispersion varies as a function of wavelength but is still moderately well described by the Sellmier-4 formula and standard parameters. However, when warm and cold CdSe samples are compared, the deviation from the Sellmeier-4 formula is of a larger magnitude and occurs at shorter wavelengths for the cold sample. Based on a normalization to 8.5 μm, we estimate the birefringence of the cold material between 8.30 to 22.84 μm. The cooling of the CdSe Wollaston prism to 30 K has little or no effect on the long-wavelength cutoff of transmission.

References

1. E. Oliva, S. Gennari, L. Vanzi, A. Caruso, and M. Ciofini, "Optical materials for near infrared Wollaston prisms," *Astron. Astrophys. Suppl. Ser.* **123**, 179–182 (1997).
2. M. Tamura, M. Fukagawa, H. Kimura, T. Yamamoto, H. Suto, and L. Abe, "First two-micron imaging polarimetry of β Pictoris," *Astrophys. J.* **641**, 1172–1177 (2006).
3. A. Chrysostomou, J. H. Hough, M. G. Burton, and M. Tamura, "Twisting magnetic fields in the core region of Orion Molecular CLOUD-1," *Mon. Not. R. Astron. Soc.* **268**, 325–334 (1994).
4. R. R. J. Antonucci and J. S. Miller, "Spectropolarimetry and the nature of NGC 1068," *Astrophys. J.* **297**, 621–632 (1985).
5. J. H. Hough, "Polarimetry: a powerful diagnostic tool in astronomy," *Astron. Geophys.* **47**(3), 31–35 (2006).
6. A. C. H. Glasse, E. I. Atad-Ettedgui, and J. W. Harris, "Michelle midinfrared spectrometer and imager," *Proc. SPIE* **2871**, 1197–1203 (1997).
7. C. Packham, S. Young, S. Fisher, K. Volk, R. Mason, J. H. Hough, P. F. Roche, M. Elitzur, J. T. Radomski, and E. Perlman, "Gemini mid-IR polarimetry of NGC 1068: polarized structures around the nucleus," *Astrophys. J. Lett.* **661**, 29–32 (2007).
8. C. C. Packham, D. J. Axon, J. H. Hough, T. J. Jones, P. F. Roche, M. Tamura, and C. M. Telesco, "Mid-IR polarimetry: new vistas for SOFIA," *Bull. Am. Astron. Soc.* **39**, 746 (2007).
9. C. C. Packham, D. J. Axon, J. H. Hough, T. J. Jones, P. F. Roche, M. Tamura, and C. M. Telesco, "Design of a mid-IR polarimeter for SOFIA," *Proc. SPIE* **7014**, 70142H (2008).
10. C. M. Telesco, D. Ciardi, J. French, C. Ftaclas, K. T. Hanna, D. B. Hon, J. H. Hough, J. Julian, R. Julian, M. Kidger, C. C. Packham, R. K. Pina, F. Varosi, and R. G. Sellar, "CanariCam: a multimode mid-infrared camera for the Gran Telescopio CANARIAS," *Proc. SPIE* **4841**, 913–922 (2003).
11. C. Packham, J. H. Hough, L. Kolokolova, and C. M. Telesco, "Plarimetry research at the University of Florida," *J. Quant. Spectrosc. Radiat. Transf.* **88**, 285–295 (2004).
12. C. Packham, C. M. Telesco, J. H. Hough, and C. Ftaclas, "CanariCam: the multimode mid-IR instrument for the GTC," *Rev. Mex. Astron. Astrofis.* **24**, 7–12 (2005).
13. M. Bass, Ed., *Handbook of Optics*, vol. 2, Optical Society of America, Washington DC (1994).
14. J. H. Hough, A. Chrysostomou, and J. A. Bailey, "A new imaging infrared polarimeter," *Exp. Astron.* **3**, 127–129 (1994).
15. D. B. Chenault and R. A. Chipman, "Infrared birefringence spectra for cadmium sulfide and cadmium selenide," *Appl. Opt.* **32**(22), 4223–4227 (1993).
16. S. Sako, Y. K. Okamoto, H. Kataza, T. Miyata, S. Takubo, M. Honda, T. Fujiyoshi, T. Onaka, and T. Yamashita, "Improvements in operating the Raytheon 320×240 pixel Si:As impurity band conduction mid-infrared array," *Publ. Astron. Soc. Pac.* **115**, 1407–1418 (2003).
17. D. Beasley, personal communication (2008).

Christopher Packham is an associate scientist in the Department of Astronomy in the University of Florida. He received both his BSc and PhD in astronomy from the University of Hertfordshire (UK). He was a Royal Society/MONBUSHO Fellow at the National Astronomical Observatory Japan in 1996, and was subsequently a support astronomer at the Isaac Newton Group of Telescopes (Spain) until moving to Florida in 2000. His main research areas are that of IR instrument development, especially polarimetry, and the application of those instruments to investigations of centers of so-called active galactic nuclei.

Rachel E. Mason is a science fellow at the Gemini Observatory where her duties include supporting users of Gemini's mid-IR instrumentation. Following a PhD in astronomy at the Royal Observatory Edinburgh, she worked for the NOAO Gemini Science Center in Tucson and La Serena, Chile, before moving to Gemini in 2006. Research topics of particular interest include the nature and origin of the putative torus of AGN unified models and its relation to the AGN host galaxy. Her recent publications have demonstrated the utility of sub-arcsecond spatial resolution mid-IR spectroscopy in providing high quality data against which to test new torus models, and provided evidence that star formation may make an important contribution to the nuclear obscuration in some galaxies.

Glenn D. Boreman is Trustee Chair Professor of Optics at University of Central Florida, CREOL. he received his BS in optics from the University of Rochester, and his PhD in optics from the University of Arizona. he has been a visiting scholar at Imperial College in London, Swiss Federal institute of Technology (ETH) in Zürich, Complutense University in Madrid, and FOI in Linköping, Sweden. He served as editor-in-chief of OSA's journal *Applied Optics*. He is co-author of *Infrared Detectors and Systems*, and author of *Modulation Transfer Function in Optical and Electro-Optical Systems* and *Basic Electro-Optics for Electrical Engineers*. He is a fellow of SPIE, OSA, and the Military Sensing Symposium.